Nanometre resolution investigations of facet displacement during the single crystal growth using the real/time analysis of full two-dimensional digitised interferograms

D. Lovrić, Z. Vučić, J. Gladić, S. Mitrović, M. Milas and N. Demoli

Institute of Physics, Bijenička 46, P.O.B. 304, 10001 Zagreb, Croatia

Introduction

We have monitored *in situ* the growth of nonstoichiometric cuprous selenide spherical single crystals of equilibrium-like shape at fixed temperature of around 800 K, at fixed stoichiometry and fixed chemical potential difference between the surface of the growing crystal and the source of copper atoms /1/. Our crystal has grown within the sealed cylindrical ampoule which has been placed uniaxially within the tubular transparent furnace. The stability and homogeneity of the temperature in the growth region is very important and has been kept constant within ±0.25 K. The growth process has been slow, with constant volume growth rate $dV/dt=0.01\ mm^3/h$, yielding radial velocities ranging between 15 and .3 nm/s. These crystals are ones of the very few known which exhibit ECS at almost millimetre sizes. At these temperatures the surface of these crystals exhibits atomically smooth facets separated by atomically rough rounded parts. The growth method has provided spherical single crystal with well developed (111) facets of cubooctahedral symmetry. Our aim has been the investigation of new growth modes in as wide range of growth rates as possible. We were to some extent motivated by the recently discovered so called burst-like mode of growth of ^4He single crystals at the temperatures in the range between 2mK and 250 mK, which was found using the pressure difference measurements, rather than the interferometric measurements /2/. We need as precise measurements as possible since we are interested in studying the dynamics of the surface objects structure and correlating this structure to the microscopic balance of forces in the vicinity of the facet boundary using the model of stepped surface with repulsive step interactions. Therefore, we need the measurements with nanometre resolution, which can detect very small facet displacements.

1 Digital interferometry

As a suitable method for noncontact measurements of object displacements, we have chosen digital interferometry (DI) method. DI combines advantages of the interferometric sensitivity with computer processing by using a CCD camera. The CCD detector is converting optical fringe patterns first into electronic, and then into numerical data. Drawback of the method is still relatively large pixel size of the CCD detector area which implies the use of low numerical aperture configurations. In studying microscopic objects, DI was used for the determination of the resonant frequencies and mode shapes of vibrating atomic force microscope tips /3/.

A schematic representation of our interferometer is shown in Fig. 1. The crystal was illuminated by the light of a Spectra-Physics 25 mW He-Ne laser (wavelength: 632.8 nm). An enlarged image of the facet was formed by an objective and captured by the CCD camera. We have placed a polarizer between the objective and CCD camera in order to select only polarization component of the light coming from the facet identical to the polarization of the

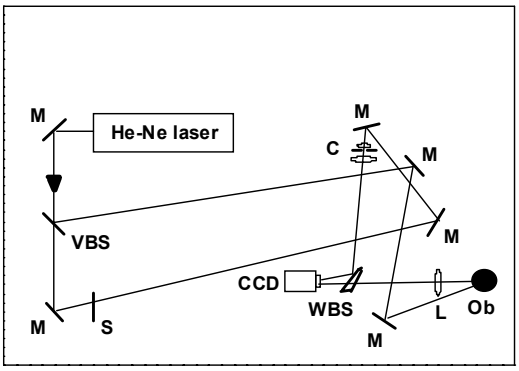

Fig. 1. Scheme of the interferometric setup: M, mirror; VBS, variable beam splitter; S, shutter; C, collimator; WBS, wedge beam splitter; L, lens; Ob, object.

reference beam. The reference beam was expanded by a spatial filter device and directed to the CCD camera by a wedge beam splitter. The interferometric setup is analogous to an electronic speckle pattern interferometer with a distinctive feature: the facet of the single crystal was optically flat most of the time of monitoring, and thus the speckled image of the facet was essentially specular. The interferometer, aligned on a vibration isolated table, was isolated from the furnace device, and completely covered, to prevent air convection. A special care was devoted to the control of all optical parameters as well as to the crystal growth conditions.

2 Analysis of interferograms

The recorded interference fringes have then been grabbed from the videotapes and analysed. We have chosen our frame-taking rate to be 25 frames per second since we wanted to increase the range of accessible growth rates as much as possible. Such high frame-taking rate has turned out to be necessary as well, because of the mechanical vibrations occurring during the growth.

We have analysed the full two-dimensional digitised frames, i.e. interferograms (256 grey levels), on a square grid of 64*64 pixels. We have used and refined the Fourier-transform method of analysing fringe-patterns of the general form /4/:

$$g(\mathbf{r}) = a(\mathbf{r}) + b(\mathbf{r})\cdot\cos[2\pi\mathbf{q}\cdot\mathbf{r} + \Phi(\mathbf{r})],$$

in which the desired information is contained in the phase field $\Phi(\mathbf{r})$, while $a(\mathbf{r})$ and $b(\mathbf{r})$ are the functions whose spatial dependencies originate from the imperfections of the measurements, and $\mathbf{r}=(x,y)$. The basic assumption of the method is that $\Phi(\mathbf{r})$, $a(\mathbf{r})$ and $b(\mathbf{r})$ are spatially slow varying functions on the scale established by the spatial-carrier frequency $\mathbf{q}=(q_x,q_y)$, which is given by the number of pixels per interference line. If this assumption is fulfilled, the Fourier spectrum contains features that are separated by $\mathbf{q}$. The standard procedure /4/ proceeds by extracting out one of the first order maxima, centred either at $\mathbf{q}$ or $-\mathbf{q}$, and shifting it to the origin of the inverse space. After the inverse Fourier transform back to the real space, it is straightforward to extract the desired information, i.e. the phase field $\Phi(\mathbf{r})$.

The first thing one may think about in order to enhance the quality of interferograms is the background subtraction. Since we have been dealing with a very large number of frames (72 hours of continuous frame taking during the crystal growth, at the rate of 25 frames per second), some method of automatic background subtraction is mandatory. If the interferograms were “perfect”, one would expect that by adding up a certain number of subsequent interferograms an image without any interference lines would appear, and one might take this

image as the background. The only prominent feature in the Fourier spectrum of such an image would be a zero order peak. Our method of "running background" subtraction is based on these considerations. Since we may not expect a perfect cancellation of interference pattern, we have established the following criterion. After each addition of a single frame, we have Fourier analysed the sum and found the ratio of first to zero order peak intensity. As long as this ratio, as a function of the number of frames added, diminishes, the frame added contributes to the disappearing of the interference pattern. When by adding n+1 frame the trend of diminishing of this ratio stops, we have pronounced the sum of n frames the "running background" and have subtracted it from each of the n frames. The $(n+1)^{st}$ frame has then been taken as the first in the new sequence of frames that would define the subsequent background image. By doing this we have been able to enhance the first to zero order peak intensity ratio (i.e. the signal to "noise" ratio) by more than two orders of magnitude. This would prove particularly useful in analysing the interferograms for which the carrier frequency is smaller, i.e. for which the first order peaks overlap with the zero order one. Moreover, such background subtraction enables the extraction of one of the first order maxima to be much more straightforward, i.e. it may be done without the introduction of Gaussian (or some other) window centred at the position of the first maximum in $|g(\mathbf{q})|$. In Fig.2 we plot the Fourier spectrum $|g(\mathbf{q})|$ of a typical frame without and with the subtraction of the background.

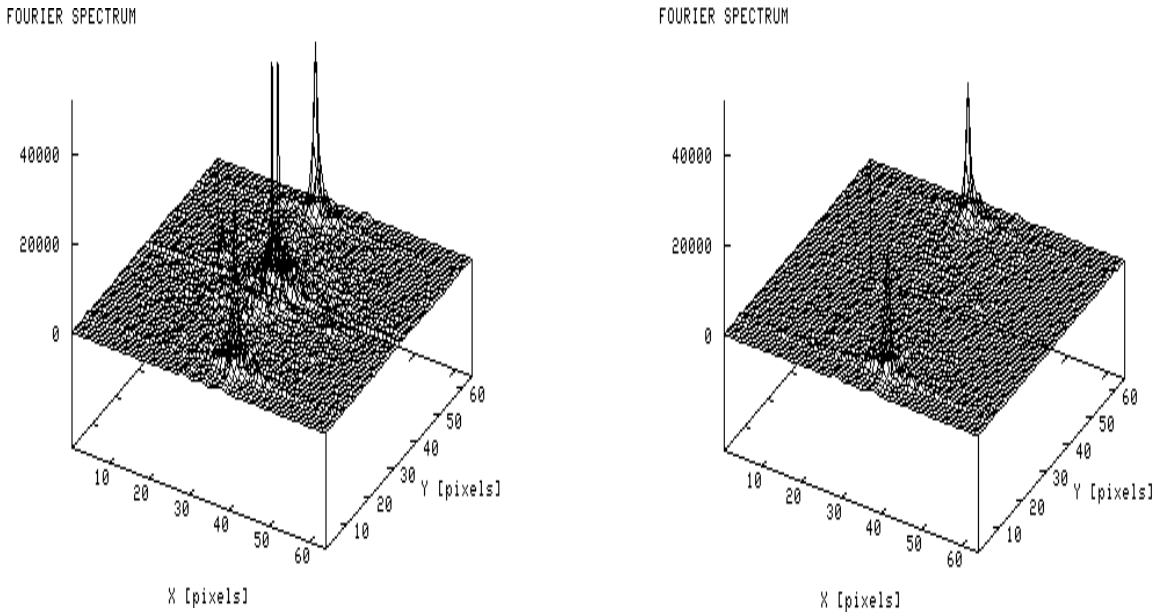

Fig.2. Fourier spectra of a typical frame. Left: FT of raw data, right: FT of the same frame after the background has been subtracted. X and Y denote components of **q**.

The above mentioned procedure of shifting one of the first order peaks into the origin of the spatial frequency space is straightforward and exact if the carrier frequency has integer components expressed in pixels, $\mathbf{q}=\mathbf{q_0}=(q_{0x}, q_{0y})$ The optics of the experimental set-up usually yields non-integer pixel components of **q**, i.e. $\mathbf{q}=\mathbf{q_0}+\delta$, where $|\delta_x, \delta_y| \leq 0.5$, and that was the case in our measurements. The problem then consists in finding the deviation δ of the carrier frequency from the nearest pixels in the spatial frequency space. We have made use of the sampling theorem /5/, which states that a continuous function, sampled at an interval Δ and bandwidth limited to frequencies smaller than the Nyquist critical frequency $1/(2\Delta)$ is

completely determined by its samples. We have applied this theorem in the spatial frequency space, to the amplitude of the Fourier transform $|g(\mathbf{q})|$, $\mathbf{q}=(q_x,q_y)$, which is a well behaved function in the frequency space. Explicitly, one has the following ("exact" interpolation) formula:

$$|g(q_x,q_y)| = \Delta q_x \Delta q_y \sum_{m,n} |g_{m,n}| \frac{\sin[\pi(q_x/\Delta q_x - m)]}{\pi(q_x/\Delta q_x - m)} \cdot \frac{\sin[\pi(q_y/\Delta q_y - n)]}{\pi(q_y/\Delta q_y - n)},$$

where $|g_{m,n}|$ stands for $|g(q_x = m\cdot\Delta q_x, q_y = n\cdot\Delta q_y)|$. By making use of this formula, one has to calculate $|g(\mathbf{q})|$ on the grid limited by $|\delta_x, \delta_y| \le 0.5$ around the integer-pixel point $\mathbf{q_0}$, and obtain its values to the chosen sub pixel accuracy. The maximum of these values defines δ, i.e. the deviation of the carrier frequency components from the integer pixel values.

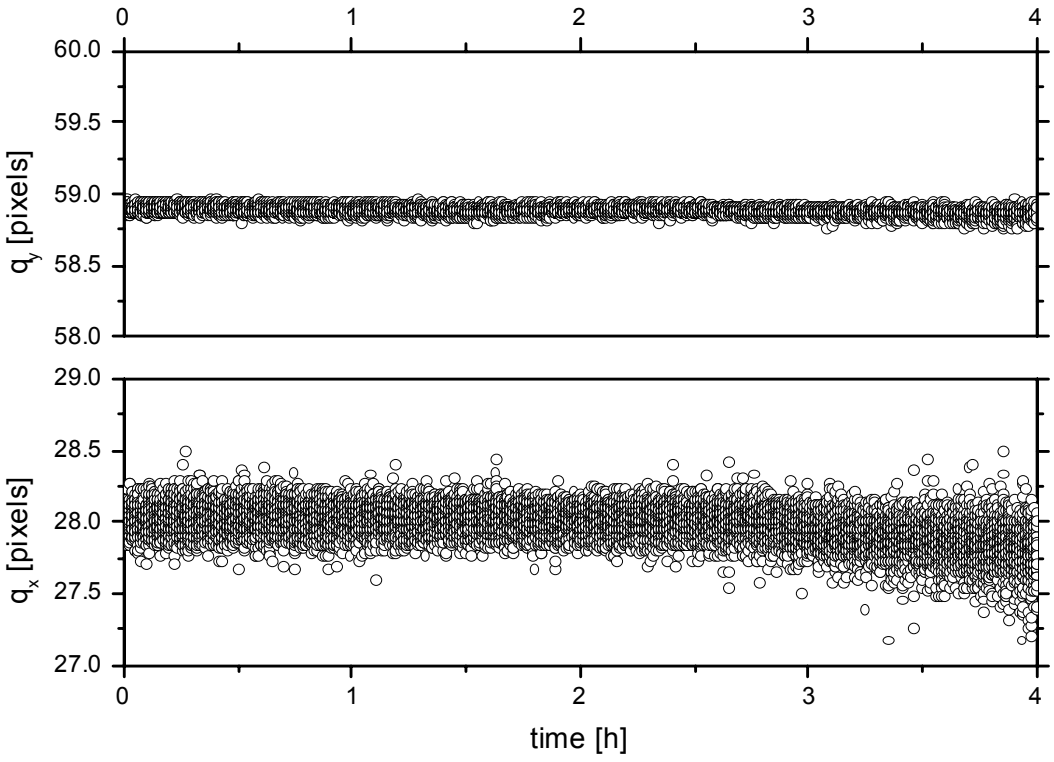

Fig. 3. x (lower panel) and y (upper panel) components of the spatial carrier frequency $\mathbf{q}=\mathbf{q_0}+\delta$ which maximize the first maximum of the Fourier spectrum $|g(\mathbf{q})|$.

In Fig. 3 we plot the components q_x and q_y of the spatial carrier frequency for which $|g(\mathbf{q})|$ acquires its maximum value as a function of time for first four hours of monitored growth. We shift now the chosen first order maximum to the origin of the spatial frequency space by the integer values $\mathbf{q_0}$, and upon the inverse Fourier transformation we obtain $G_0(\mathbf{r})$, which defines the uncorrected phase field $\Phi_0(r)$. By expanding $g(\mathbf{q})$, which is, owing to the "noise" contributions a and b, a continuous function of $\mathbf{q}$, in Taylor series around $\mathbf{q_0}$, and by performing the inverse Fourier transform, one obtains, as expected, for the correction arising from the sub pixel correction δ to $\mathbf{r}$:

$$\Delta G(\mathbf{r})=\exp(i\delta\cdot\mathbf{r}),$$

and the corrected value of the inverse transform reads

$$G(\mathbf{r})=G_0(\mathbf{r})\cdot\exp(i\delta\cdot\mathbf{r}).$$

It is now straightforward to calculate from $G(\mathbf{r})$ the corrected phase field $\Phi(\mathbf{r})$.
We have tested the above described procedure on test functions involving non-integer components of the carrier frequency, and obtained phase field with the accuracy better than 1%, independent of the value of (predefined) phase field, which enables the determination of facet displacement with the theoretical resolution better than 2 nm.
In Fig.4 we plot the phase fields $\Phi(\mathbf{r})$ for two typical consecutive frames, and their difference $\Delta\Phi(\mathbf{r})$. All of the phase fields have been unwrapped by the standard procedure /6/.

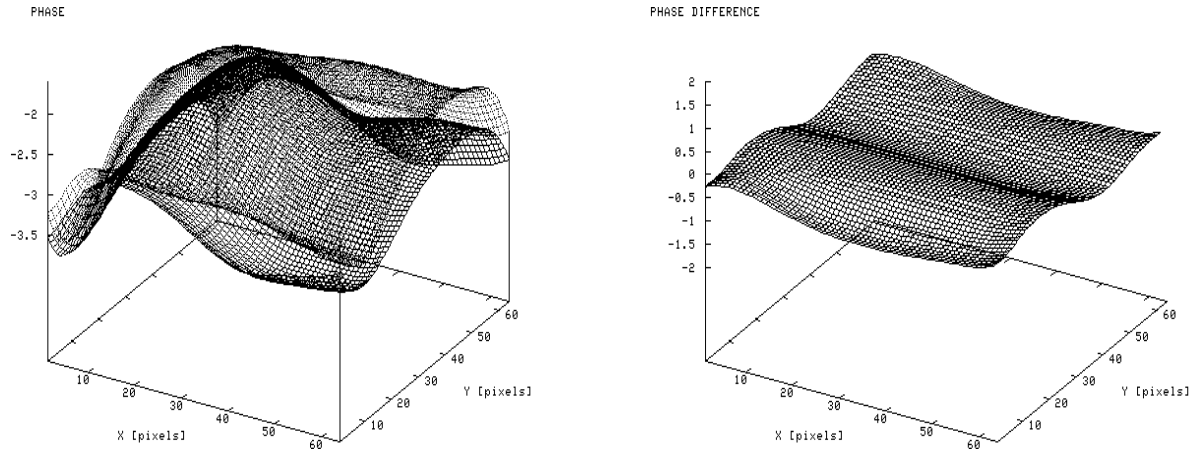

Fig.4. Phase fields $\Phi(\mathbf{r})$ of two consecutive frames (left panel), and their difference (right panel).

The facet displacement between two consecutive frames is given by:

$$\overline{\Delta h}=\overline{\Delta\Phi}\cdot\frac{\lambda}{4\pi}\cdot\frac{1}{\cos(\theta/2)},$$

where λ is the wavelength of the laser beam used (λ=632.8nm), θ is the angle between the incoming laser beam and the beam reflected from the facet, and $\overline{\Delta\Phi}$ is the phase difference $\Delta\Phi(\mathbf{r})$ averaged over the central part of the grid in real space.

3 Results

In Fig.5 we plot the cumulative facet displacement, i.e. the facet height as a function of time, for first four hours of monitored facet growth. We plot here as well, with the bold line, the same curve from which the high frequency features, originating mainly from the experimental noise and happening on the scale shorter that 15 minutes, have been removed. From this curve one may notice a growth mode of our crystal in which the intervals of fast growth (the growth rate being up to ≈15 nm/s) are separated by intervals of very slow growth (the growth rate

falling to ≈0.3 nm/s). The detailed analysis of the obtained results, for much longer interval of growth, will be presented elsewhere /7/.

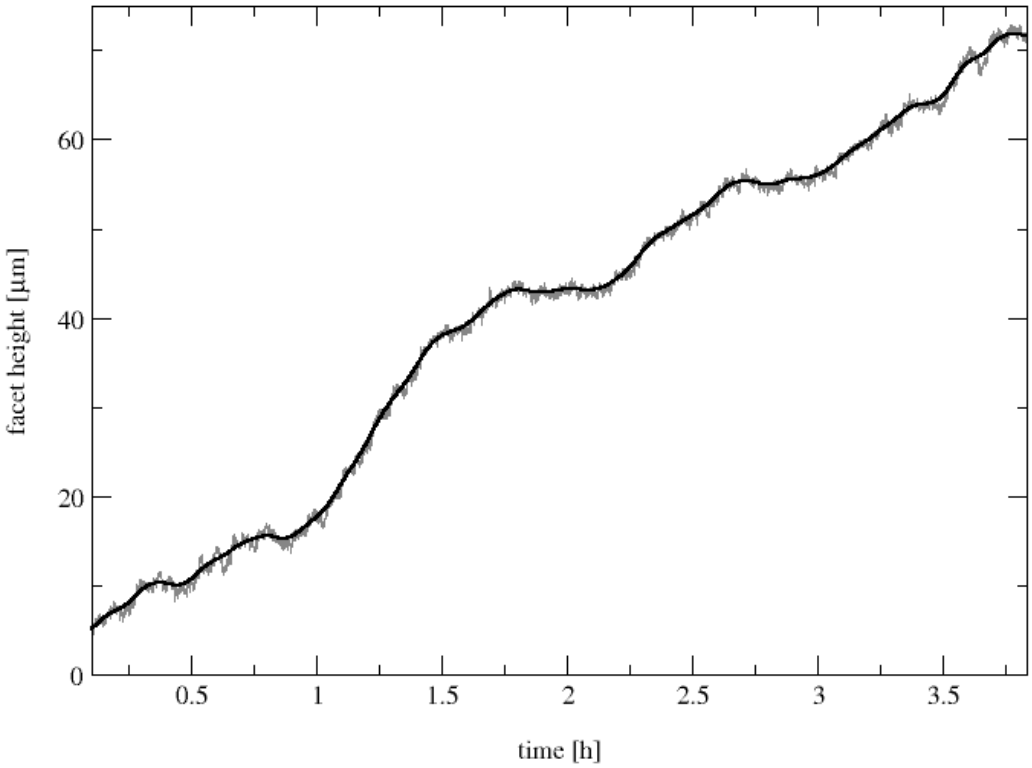

Fig. 5. Single line: Facet height as a function of time. Bold line: The same curve upon the removal of features corresponding to time scale shorter than 15 minutes.

References

/1/ Vučić Z., Gladić J., Growth rate of equilibrium-like-shaped single crystals of superionic conductor cuprous selenide, J. Crystal Growth 205(1999)136-152.

/2/ Ruutu J.P., Hakonen P.J., Babkin A.V., Parshin A.Ya., Penttilä J.S., Saramäki J.P., Tvalashvili G.: Facet growth of 4He crystals at mK temperatures, Phys. Rev. Lett. 76(1996)22, 4187-4190.

/3/ G. C. Brown, R. J. Pryputniewicz: Holographic microscope for measuring displacements of vibrating microbeams using time-averaged, electro-optic holography, Opt. Eng. 37 (1998)5, 1398-1405.

/4/ Takeda M., Ina H., Kobayashi S.: Fourier-transform method of fringe-pattern analysis for computer-based topography and interferometry, J. Opt. Soc. Am. 72(1982)1, 156-160.

/5/ See for example Press W.H., Teukolsky S.A., Vetterling W.T., Flannery B.P, Numerical Recipes, Cambridge University Press, 1992, ch. 12.

/6/ Macy, W.W. Jr: Two-dimensional fringe-pattern analysis, Appl. Opt. 22(1983)3898.

/7/ D. Lovrić, Z. Vučić, J. Gladić, S. Mitrović, M. Milas and N. Demoli, to be published.